Supporting Information

Liquid crystalline 2-thienyl-4,6-diamino-1,3,5-triazines exhibiting $Im\overline{3}m$ and $Pm\overline{3}n$ micellar cubic phases in an inverted sequence

Heng Dai ,[a] Xueyan Yang,[a] Xiaoping Tan,[a] Fawu Su [a], Xiaohong Cheng, * [a] Feng Liu,*[b] Carsten Tschierske*[c]

[a] Prof. Dr. X. H. Cheng, H. Dai, X. Y. Yang, X. P. Tang, F.W. Su
Chemistry Department
Yunnan University
Kunming, Yunnan 650091, P. R. China
Fax: (+86) 871 65032905
E-mail: xhcheng@ynu.edu.cn

[b] Prof. Dr. F. Liu
State Key Laboratory for Mechanical Behavior of Materials
Xi’an Jiaotong University
Xi’an, P. R. China, 710049
Fax: (+86) 29 82663453
E-mail: feng.liu@mail.xjtu.edu.cn

[c] Prof. Dr. C. Tschierske
Institute of Chemistry Organic Chemistry
Martin-Luther University Halle-Wittenberg
Kurt-Mothes Str. 2, 06120 Halle/Saale, Germany
Fax: (+49) 345 55 27346
E-mail: carsten.tschierske@chemie.uni-halle.de

Content

1. Additional Experimental Data

1.1 Experimental techniques

High-resolution small-angle powder diffraction experiments were recorded on station BL16B1 at Shanghai Synchrotron Radiation Facility (SSRF), China. Samples were held in evacuated 1 mm capillaries. A modified Linkam hot stage with a thermal stability within 0.2 ºC was used, with a hole for the capillary drilled through the silver heating block and mica windows attached to it on each side. A MarCCD 165 detector was used. q calibration and linearization were verified using several orders of layer reflections from silver behemate and a series of n-alkanes. Positions and intensities of the diffraction peaks were measured using PeakSolve^{TM} (Galactic).

The 3-d electron density maps were reconstructed on the basis of the general Eqn. (1), using the relative electron densities $I(hkl)$:

$$E(xyz) = \Sigma_{hkl}\ \mathrm{sqrt}[I(hkl)]\ \exp[\mathrm{i}2\pi(hx+ky+lz)+\phi_{hkl}] \qquad \text{(Eqn. 1)}$$

for 2D structures $I(hk)$ and Eqn. (2) were used:

$$E(xy) = \Sigma_{hk}\ \mathrm{sqrt}[I(hk)]\ \exp[i2\pi(hx+ky) +\phi_{hk}] \qquad \text{(Eqn. 2)}$$

For the centro-symmetric structures considered in this work the phase angle ϕ can take up the values of 0 or π. The choice of a phase combination was initially made on the merit of each reconstructed electron density map obtained using the most intense reflections, combined with the additional knowledge of the molecules (molecular shape, length, volume of each part and the distribution of electron density among the different moieties).

GISAXS experiments were performed on Beamline I16 at Diamond Light source, U.K. and station BL14B1 at SSRF. Thin film samples were prepared from the melt on a silicon wafer. The film-coated 5 x 5 mm^2 Si plates were placed on top of a custom built heater, which was then mounted on a six-circle goniometer. A Pilatus 2M (Dectris) detector at Diamond and a MarCCD 225 detector at SSRF were used respectively. The sample enclosure and the beam pipe were flushed with helium.

1.2 Additional textures of LC phases and DSC traces

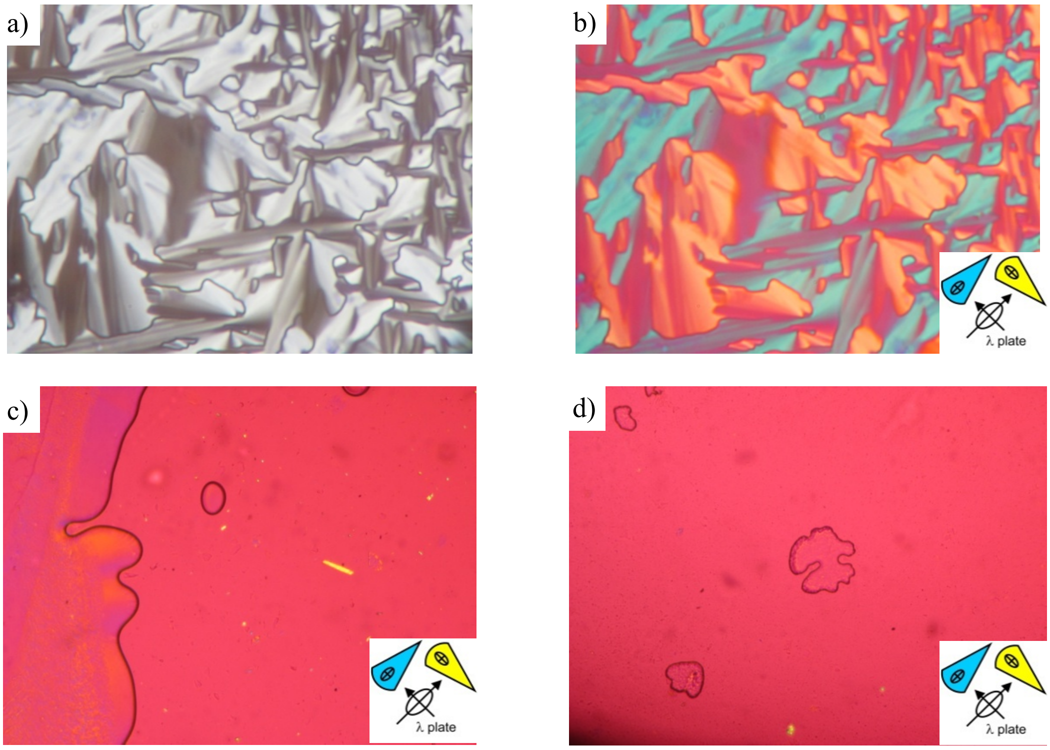

Figure S1 Representative textures between crossed polarizers: (a) $\mathrm{Col_{hex}}$ phase of **T3-10** at 120 °C; (b) same texture with λ-retarder plate (the indicatrix orientation in the compensator is shown on the right; the columnar phase is optically negative as indicated by the orientation of the blue shifted and yellow shifted fans; this means that in the columns the preferred direction of the intramolecular π-conjugation pathway - coinciding with the long axis of the aromatic cores - is on average perpendicular to the column long axis; (c, d) textures of the $\mathrm{Cub_I}$ phases of compounds **T3-12** and **T3-14**, respectively, with a λ-retarder plate, at T = 100 °C (here the λ-plate was only used to improve the contrast, otherwise the whole area would appear completely black).

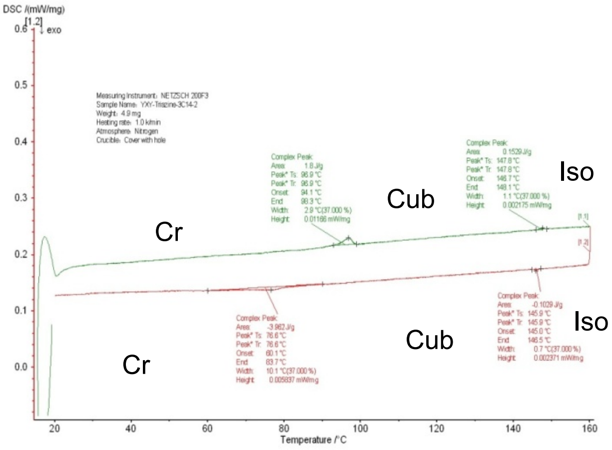

Figure S2 DSC trances of **T3-14** (1 K $\mathrm{min^{-1}}$, second scan).

1.3 Additional XRD data

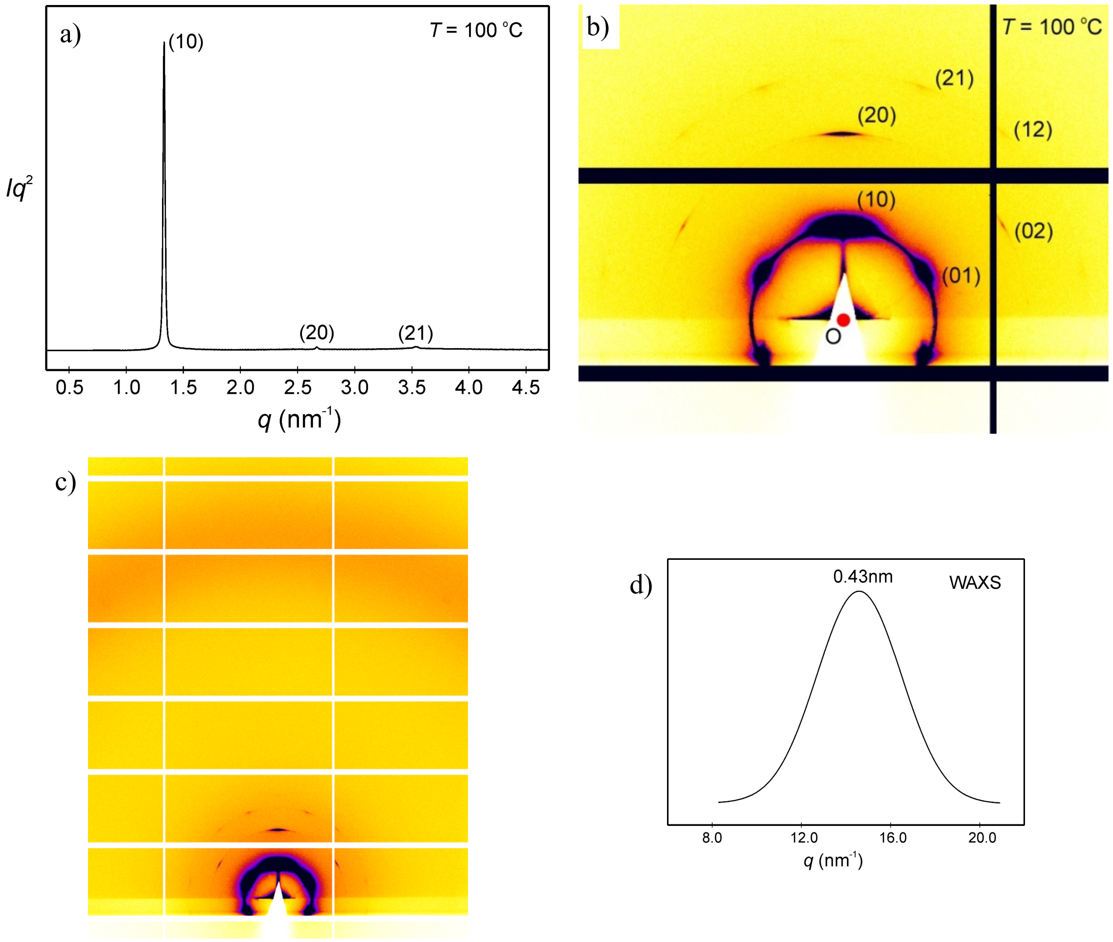

Figure S3 X-ray diffraction patterns of the Col_{hex} phase of compound **T3-10** at *T* = 100 °C (synchrotron source): a) SAXS powder diffraction pattern; b) GISAX pattern; c) GISAXS-GIWAXS pattern. The white horizontal and vertical lines are gaps between the detector elements; d) WAXS of the GISAXS-GIWAXS pattern with the *d* value for the maximum of the diffuse outer scattering.

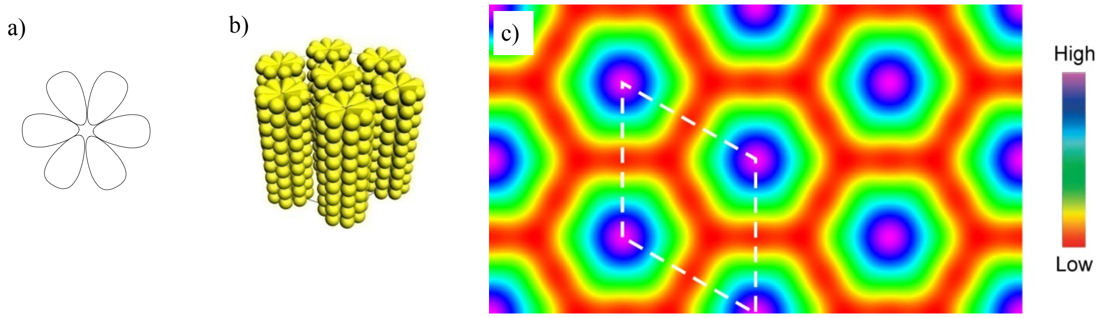

Figure S4 The $\mathrm{Col}_{hex}/p6mm$ phase of **T3-10**: a) a model showing the organizations of compounds **T3-10** in the columnar LC phase; b) schematic sketch of a rosette formed by 8 molecules in the cross section; c) reconstructed electron density map for the $\mathrm{Col}_{hex}/p6mm$ phase.

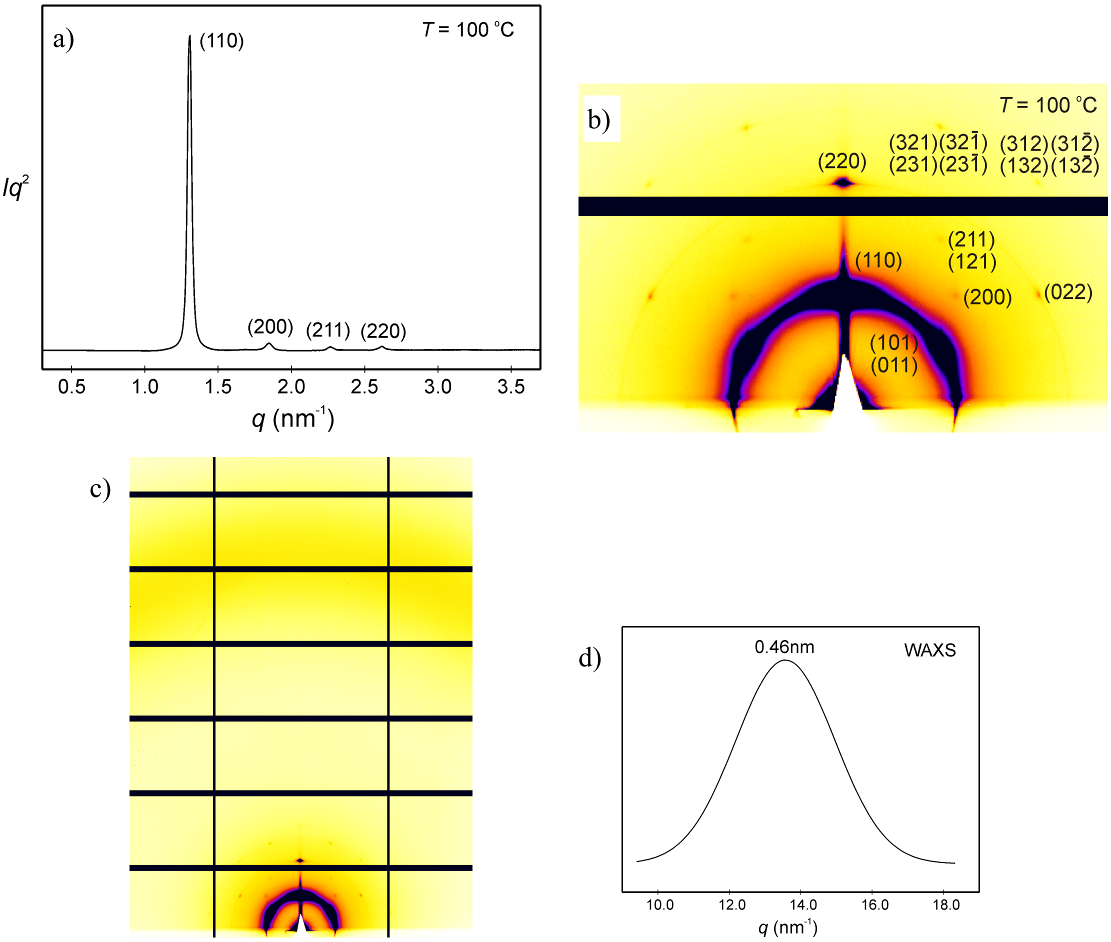

Figure S5 X-ray diffraction patterns of the Cub/$Im\bar{3}m$ phase of compound **T3-12** at T = 100 °C (synchrotron source): a) SAXS diffractogram; b) GISAXS pattern of a thin film on Si (111) surface. The LC domains are cylindrically averaged with their [110] axis along the film normal (vertical in the figure, the ‘‘fiber axis’’). Only one reflection of a Friedel pair is indicated, and reflections with $h < 0$ are omitted; c) GISAXS-GIWAXS pattern. The black horizontal and vertical lines are gaps between the detector elements; d) WAXS of the GISAXS-GIWAXS pattern with the d value for the maximum of the diffuse outer scattering.

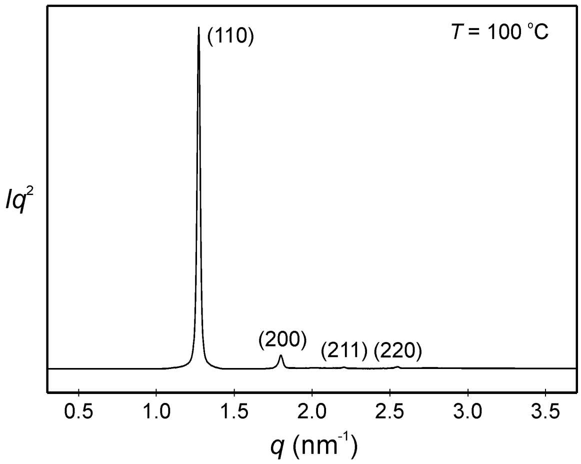

Figure S6 SAXS diffractogram of the Cub/$Im\overline{3}m$ phase of the compound **T3-16** (synchrotron source).

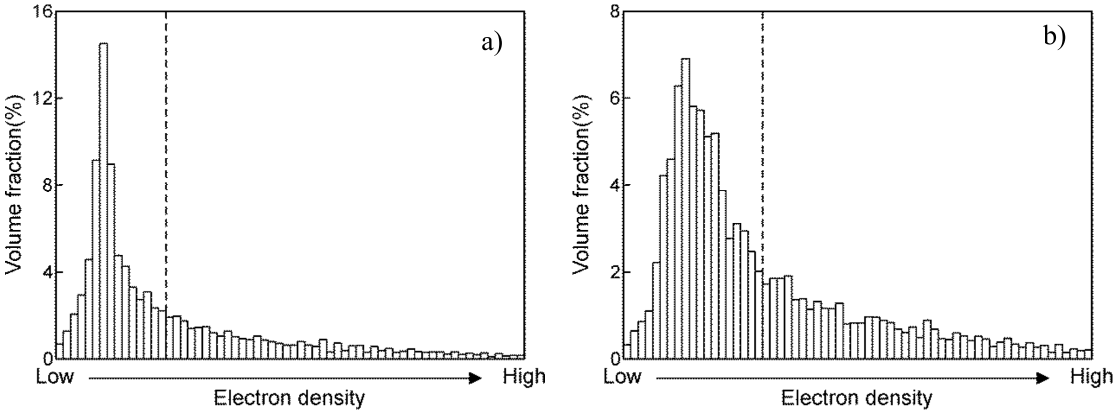

Figure S7 Histograms of the reconstructed electron density maps of compound **T3-14**: a) the Cub/$Im\overline{3}m$ phase; b) the Cub/$Pm\overline{3}n$ phase. The level of the isoelectron surface used in Figure 1b and 1d is indicated by the dashed vertical line, which corresponds to the boundary between the low-medium electron density regions (66% of total volume) and the high density polar regions (33% of total volume).

Table S1 Experimental and calculated *d*-spacing of the observed SAXS reflection of the hexagonal phase at 100 ºC of compound **T3-10**. All intensity values are Lorentz and multiplicity corrected.

(*hk*)	$d_{obs.}$ – spacing (nm)	$d_{cal.}$ – spacing (nm)	*intensity*	*phase*
(10)	4.72	4.72	100.0	0
(20)	2.36	2.36	1.0	π
(21)	1.78	1.78	0.4	0
a_{hex} = 5.45 nm				

Table S2 Experimental and calculated *d*-spacing of the observed SAXS reflection of the Cub/$Im\overline{3}m$ phase of **T3-12** at 100 ºC. All intensity values are Lorentz and multiplicity corrected.

(*hkl*)	$d_{obs.}$ – spacing (nm)	$d_{cal.}$ – spacing (nm)	*intensity*	*Phase*
(110)	4.81	4.81	100.0	0
(200)	3.40	3.40	6.2	0
(211)	2.77	2.78	0.7	0
(220)	2.40	2.41	1.5	π
a_{cub} = 6.81 nm				

Table S3 Experimental and calculated *d*-spacing of the observed SAXS reflection of the Cub/$Im\overline{3}m$ phase of **T3-14** at 100 ºC. All intensity values are Lorentz and multiplicity corrected.

(*hkl*)	$d_{obs.}$ – spacing (nm)	$d_{cal.}$ – spacing (nm)	*intensity*	*Phase*
(110)	5.04	5.04	100.0	0
(200)	3.56	3.56	6.5	0
(211)	2.91	2.91	0.4	0
(220)	2.52	2.52	0.9	π
a_{cub} = 7.13 nm				

Table S4 Experimental and calculated *d*-spacing of the observed SAXS reflection of the Cub/$Pm\bar{3}n$ phase of **T3-14** at 120 ºC. All intensity values are Lorentz and multiplicity corrected.

(*hkl*)	$d_{\text{obs.}}$ – spacing (nm)	$d_{\text{cal.}}$ – spacing (nm)	*intensity*	*Phase*
(110)	7.87	7.87	0.1	0
(200)	5.56	5.56	64.3	0
(210)	4.98	4.98	100.0	0
(211)	4.54	4.54	73.5	0
(220)	3.93	3.93	1.2	π
(310)	3.51	3.52	0.6	π
(321)	2.97	2.97	0.1	0
(400)	2.78	2.78	2.5	π
(410)	2.69	2.70	0.3	π
(330)	2.62	2.62	0.0	/
(411)			0.1	/
(420)	2.48	2.49	0.3	/
(421)	2.42	2.43	0.3	/
a_{cub} = 11.13 nm				

Table S5 Experimental and calculated *d*-spacing of the observed SAXS reflection of the Cub/$Im\bar{3}m$ phase of **T3-16** at 100 ºC. All intensity values are Lorentz and multiplicity corrected.

(*hkl*)	$d_{\text{obs.}}$ – spacing (nm)	$d_{\text{cal.}}$ – spacing (nm)	*intensity*	*Phase*
(110)	4.94	4.94	100.0	0
(200)	3.49	3.49	9.6	0
(211)	2.85	2.85	0.2	0
(220)	2.47	2.47	0.7	π
a_{cub} = 6.99 nm				

Table S6 Experimental and calculated *d*-spacing of the observed SAXS reflection of the Cub/ $Pm\overline{3}n$ phase of **T3-16** at 120 ºC.

(*hkl*)	$d_{\mathrm{obs.}}$ – spacing (nm)	$d_{\mathrm{cal.}}$ – spacing (nm)
(110)	7.68	7.68
(200)	5.43	5.43
(210)	4.85	4.85
(211)	4.43	4.43
a_{cub} = 10.85 nm		

1.4 Molecular models and calculation of packing parameters

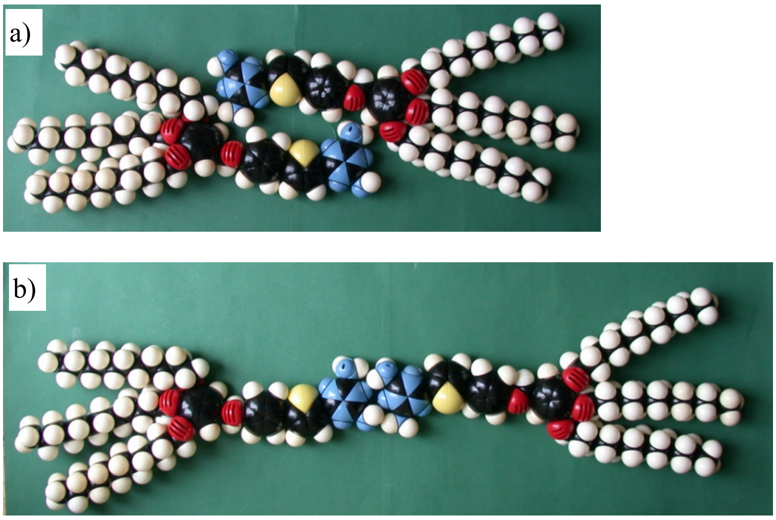

Figure S8 CPK models of compound **T3-12** showing the possible packing modes in the micellar aggregates: a) intercalated side-by-side packing leading to reduced interface curvature; b) non-intercallated end-to-end packing leading to increased interface curvature.

Table S7 Calculations of molecular volume (V_{mol}), volume of the (hypothetical) unit cells(V_{cell}) and number of molecules in these unit cells (n_{cell}).[a]

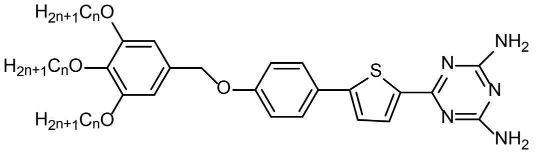

Comp	Phase	a/nm (T/°C)	micelle size D /nm	V_{cell}/nm^3	V_{mol}/nm^3	$n_{\mathrm{cell,cryst}}$	$n_{\mathrm{cell,liq}}$	n_{cell}
T3-10	Col$_{\mathrm{hex}}$	5.45 (100)	/	11.1	1.19	9.3	7.3	8.3
T3-12	$Im\bar{3}m$	6.81 (100)	5.80 (100)	315.8	1.34	236	185	210
T3-14	$Im\bar{3}m$	7.13 (100)	6.17 (100)	362.5	1.49	243	191	217
	$Pm\bar{3}n$	11.13(120)	5.57 (120)	1378.8		925	727	826
T3-16	$Im\bar{3}m$	6.99 (100)	6.05 (100)	341.5	1.64	208	164	186
	$Pm\bar{3}n$	10.85 (120)	5.43 (120)	1277.3		779	612	695

[a] $D = 0.866 \times a_{\mathrm{cub}}$ for $Im\bar{3}m$ and $0.5 \times a_{\mathrm{cub}}$ for $Pm\bar{3}n$; V_{cell} = volume of the unit cell defined by the dimensions $a_{\mathrm{hex}}^2 \times \sin(60°) \times 0.43$ nm for hexagonal phases and a_{cub}^3 for the cubic phases; V_{mol} = volume for a single molecule as calculated using the crystal volume increments;[S1] $n_{\mathrm{cell,cryst}}$ = number of molecules in the unit cell, calculated according to $n_{\mathrm{cell,cryst}} = V_{\mathrm{cell}}/V_{\mathrm{mol}}$ (average packing coefficient in the crystal is $k = 0.7$;[S2] $n_{\mathrm{cell,liq}}$ = number of molecules in the unit cell of an isotropic liquid with an average packing coefficient $k = 0.55$, calculated according to $n_{\mathrm{cell,liq}} = 0.55/0.7 \times n_{\mathrm{cell,cryst}}$; n_{cell} = in the LC phase estimated as the average of that in the $n_{\mathrm{cell,cryst}}$ and $n_{\mathrm{cell,liq}}$.

2. Syntheses and Analytical Data

2.1 General Remarks

Reactions requiring an inert gas atmosphere were conducted under argon and the glassware was oven-dried (140 °C). Commercially available chemicals were used as received. ^{1}H NMR and ^{13}C NMR spectra were recorded on a Bruker–DRX-500 ,-400 and -300 spectrometer. Elemental analysis was performed using an Elementar VARIO EL elemental analyzer. Column chromatography was performed with merck silica gel 60 (230-400 mesh). The alkoxy benzyl chlorides **6/*n*** was prepared according to literature procedure.[S3]

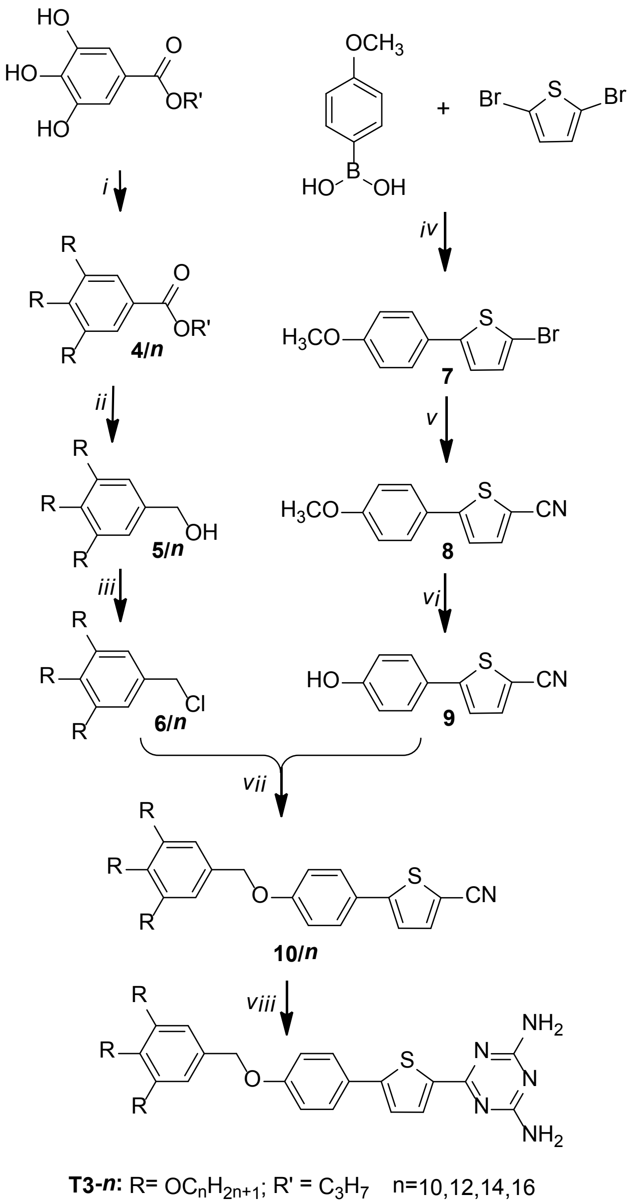

Scheme S1 Synthesis of the triazine derivatives; *Reagents and conditions*: *i*) $C_nH_{2n+1}Br$, K_2CO_3, DMF, 90℃, overnight; *ii*) $LiAlH_4$, THF, 50℃, 4h; *iii*) $SOCl_2$, DMF, THF, 5h; *iv*) $Pd(PPh_3)_4$, Na_2CO_3, toluene/H_2O(1/1), reflux, 4h; *v*) CuCN, DMF, reflux, 16 h; *vi*) BBr_3, CH_2Cl_2, 0℃-RT, 16h; *vii*) K_2CO_3, DMF, 90℃, overnight; *viii*) Dicyandiamide, KOH, 2-methoxyethanol, reflux, 16 h.

2.2 Intermediates

5-(4-Methoxylphenyl)-2-bromo-thiophene 7[S4]

2,5-Dibromothiophene (4.84 g, 20 mmol), *p*-methoxylphenylboronic acid (3.64 g, 24 mmol) and Na_2CO_3 (4.24 g, 40 mmol), were dissolved in Toluene/H_2O (1:1,60 mL), the system was then evacuated twice and back filled with N_2. $Pd(PPh_3)_4$ (116 mg，0.1 mmol) was added under an N_2 atmosphere. The reaction mixture was stirred for 30 min at RT, and then heated to reflux overnight. After the reaction was complete (TLC), the reaction mixture was cooled to RT, extracted with ethyl acetate (3 × 30 mL), washed with brine (3 × 20 mL), dried over $MgSO_4$, then the solvent was removed in *vacuo*. The residue was purified by column chromatography (petroleum ether) to yield **7** as a white solid (2.84 g, 53%, mp:110 –112 °C). ^{1}H-NMR (500 MHz, $CDCl_3$)，δ (ppm): 7.43 (d, *J* = 8.6 Hz, 2H, Ar-H), 6.99 (d, *J* = 3.9 Hz, 1H, thio-H), 6.93 (d, *J* = 3.8 Hz, 1H, thio-H), 6.90 (d, *J* = 8.7 Hz, 2H, Ar-H), 3.83 (s, 3H, CH_3).

5-(4-Methoxyphenyl)-2-cyanothiophene 8 :[S4]

To a mixture of 5-(4-methoxylphenyl)-2-bromothiophene **7** (1.35 g, 5 mmol) and CuCN (0.9 g,10 mmol) in dry DMF (20 mL), added one drop of pyridine. The reaction mixture was heated to reflux over night. After the reaction was complete (TLC), the reaction mixture was cooled to RT, added ammonia water 25mL, stirred for 1 hour, extracted with ethyl acetate (3 × 30 mL), washed with water (3 × 20 mL) and brine (3 × 20 mL) respectively, dried over $MgSO_4$, then the solvent was removed in *vacuo*. The residue was purified by column chromatography (petroleum ether: ethyl acetate = 10:1) to yield **8** as a white solid (926 mg, 86%).^{1}H-NMR (500MHz, $CDCl_3$), δ (ppm): 7.55 (1H, d, thio-H, *J* = 3.8 Hz), 7.53 (2H, d, Ar-H, *J* = 8.6 Hz), 7.16 (2H, d, thio-H, *J* = 3.9 Hz), 6.95 (2H, d, Ar-H, *J* = 8.7 Hz), 3.85 (3H, s, CH_3).

5-(4-Hydroxyphenyl)-2-cyanothiophene 9:[S4]

A flame-dried round bottomed flask with a magnetic stirring bar was charged with 5-(4-methoxylphenyl)-2-cyan-thiophene (430 mg, 2 mmol) and CH_2Cl_2 (15 mL); added two drops of BBr_3, stirred under 0°C over night. After the reaction was complete (TLC), the mixture was diluted with CH_2Cl_2 (15 mL), and H_2O was dropwise added, then the mixture was extracted with CH_2Cl_2 (3 × 20 mL), washed with brine (3 × 20 mL), dried over $MgSO_4$, the solvent was removed in *vacuo*. The residue was purified by column chromatography (petroleum ether: ethyl acetate = 2:1) to yield **9** as a yellow solid (362 mg, 90%). ^{1}H-NMR (500MHz, $CDCl_3$), δ (ppm): 7.56 (1H, d, thio-H, *J* = 4.0 Hz), 7.49 (2H, d, Ar-H, *J* = 8.6 Hz), 7.16 (2H, d, thio-H, *J* = 3.7 Hz), 6.89 (2H, d, Ar-H, *J* = 8.6 Hz), 5.07 (1H, s, OH).

2.3 Synthesis of the 5-[4-(3,4,5-trialkoxybenzyloxy)phenyl]-2-cyanothiophenes 10/*n*

General procedure

A flame-dried round bottomed flask with a magnetic stirring bar was charged with K_2CO_3 (2 mmol), the appropriate phenol **9** (1 mmol) in dry DMF (20 mL), the reaction mixture was heated to 80°C, then the appropriate benzyl chloride **6/n** (1.1 mmol) was added under an N_2 atmosphere, then heated to 90°C , stirred over night. After the reaction was complete (TLC), the reaction mixture was cooled to RT, extracted with ethyl acetate (3 × 25 mL), washed with water (3 × 25 mL) and brine (25 mL) respectively, dried over $MgSO_4$, then the solvent was removed in *vacuo*. The residue was purified by column chromatography (petroleum ether: ethyl acetate = 2:1), Yield: 61-77%, for analytical data see Table S8.

Table S8 ^{1}H NMR data of compounds **10/*n***

10/10	Pale yellow solid；yield：471 mg, 62%；^{1}H-NMR (500MHz, $CDCl_3$), δ (ppm): 7.55 (1H, d, *thio*-H, *J* = 3.7 Hz), 7.52 (2H, d, Ar-H, *J* = 8.6 Hz), 7.16 (1H, d, *thio*-H, *J* = 3.7 Hz), 7.01 (2H, d, Ar-H, *J* = 8.5 Hz), 6.61 (2H, s, Ar-H), 4.99 (2H, s, $ArCH_2O$), 3.99-3.94 (6H, m, $3ArOCH_2$), 1.81-1.73 (6H, m, 3 $ArOCH_2C\mathbf{H}_2$), 1.47-1.27 (42H, m, $21CH_2$), 0.88 (9H, t, $3CH_3$, *J* = 6.1 Hz).
10/12	Pale yellow solid；yield：650 mg, 77%；^{1}H-NMR (500MHz, $CDCl_3$), δ (ppm): 7.56 (1H, d, *thio*-H, *J* = 3.9 Hz), 7.53 (2H, d, Ar-H, *J* = 8.7 Hz), 7.17 (1H, d, *thio*-H, *J* = 3.8 Hz), 7.02 (2H, d, Ar-H, *J* = 8.6 Hz), 6.62 (2H, s, Ar-H), 4.99 (2H, s, $ArCH_2O$), 3.99-3.94 (6H, m, $3ArOCH_2$), 1.82-1.73 (6H, m, $3ArOCH_2C\mathbf{H}_2$), 1.47-1.26 (54H, m, $27CH_2$), 0.89 (9H, t, $3CH_3$, *J* = 6.5 Hz).
10/14	Yellow solid；yield：556 mg, 61%；^{1}H-NMR (500MHz, $CDCl_3$), δ (ppm): 7.56 (1H, d, *thio*-H, *J* = 3.8 Hz), 7.53 (2H, d, Ar-H, *J* = 8.7 Hz), 7.16 (1H, d, *thio*-H, *J* = 3.8 Hz), 7.01 (2H, d, Ar-H, *J* = 8.7 Hz), 6.61 (2H, s, Ar-H), 4.99 (2H, s, $ArCH_2O$), 3.99-3.93 (6H, m, $3ArOCH_{2,}$), 1.81-1.72 (6H, m, $3ArOCH_2C\mathbf{H}_2$), 1.47-1.26 (66H, m, $33CH_2$), 0.88 (9H, t, $3CH_3$, *J* = 6.3 Hz).
10/16	Yellow solid；yield：749 mg, 74%；^{1}H-NMR (500MHz, $CDCl_3$), δ (ppm): 7.55 (1H, d, *thio*-H, *J* = 3.9 Hz), 7.52 (2H, d, Ar-H, *J* = 8.3 Hz), 7.16 (1H, d, *thio*-H, *J* = 3.6 Hz), 7.01 (2H, d, Ar-H, *J* = 8.5 Hz), 6.61 (2H, s, Ar-H), 4.99 (2H, s, $ArCH_2O$), 3.99-3.94 (6H, m, $3ArOCH_2$), 1.80-1.71 (6H, m, $3ArOCH_2C\mathbf{H}_2$), 1.47-1.26 (78H, m, $39CH_2$), 0.88 (9H, t, $3CH_3$, *J* = 6.4 Hz)

2.4 Compounds T3-*n*

General procedure: Compound **10/*n*** (0.5 mmol), KOH (0.084 g, 1.5 mmol), dicyandiamide (1.5 mmol) were dissolved in ethylene glycol monomethyl ether, the reaction mixture was heated to 120 °C and refluxed over night. After the reaction was complete (TLC), the mixture was cooled to RT, diluted with 20 mL H_2O, filtered and the solvent was removed *in vacuo*. The residue was dissolved in ethyl acetate and washed with brine. The organic extracts were concentrated and the resulting residue was purified by column chromatography (petroleum ether: ethyl acetate = 1:1). Yield: 58 - 94%, for analytical data see Table S9.

Table S9 ^{1}H NMR data of compounds **T3-*n***

T3-10	Yellow solide；yield： 397 mg, 94%；^{1}H-NMR (500MHz, CDCl$_3$), δ (ppm): 7.91 (1H, d, Thio-H, *J* = 3.7 Hz), 7.60 (2H, d, Ar-H, *J* = 8.7 Hz), 7.24 (1H, d, Thio-H, *J* = 3.8 Hz), 6.99 (2H, d, Ar-H, *J* = 8.7 Hz), 6.62 (2H, s, Ar-H), 5.28 (4H, s, 2NH$_2$), 4.98 (2H, s, ArCH$_2$O), 3.99-3.93 (6H, m, 3ArOCH$_2$), 1.82-1.72 (6H, m, 3ArOCH$_2$C**H**$_2$), 1.47-1.27 (42H, m, 21CH$_2$), 0.88 (9H, t, 3CH$_3$, *J* = 6.4 Hz). ^{13}C-NMR (125MHz, CDCl$_3$), δ (ppm): 168.4, 167.1, 159.6, 153.8, 150.2, 139.7, 138.6, 132.0, 131.8, 127.8, 127.4, 123.5, 115.8, 106.7, 73.9, 70.9, 69.5, 32.9-23.1 (multi-carbon in alkyl chain), 14.6. Elemental analysis calcd (%) for $C_{50}H_{77}N_5O_4S$ (844.2); C 71.13, H 9.19, N 8.30; Found: C 71.25, H 9.17, N 8.28.
T3-12	Yellow solide；yield：325 mg, 70%；^{1}H-NMR (300MHz, CDCl$_3$), δ (ppm): 7.92 (1H, d, Thio-H, *J* = 3.9 Hz), 7.61 (2H, d, Ar-H, *J* = 8.4 Hz), 7.23 (1H, d, Thio-H, *J* = 3.9 Hz), 7.01(2H, d, Ar-H, *J* = 9.0 Hz), 6.62 (2H, s, Ar-H), 5.19 (4H, s, 2NH$_2$), 4.98 (2H, s, ArCH$_2$O), 3.99-3.92 (6H, m, 3ArOC**H**$_2$), 1.84-1.70 (6H, m, 3ArOCH$_2$C**H**$_2$), 1.46-1.26 (54H, m, 27CH$_2$), 0.88 (9H, t, 3C**H**$_3$, *J* = 6.3Hz). ^{13}C-NMR (125MHz, CDCl$_3$), δ (ppm): 168.1, 167.2, 159.2, 153.4, 149.5, 139.6, 138.3, 131.6, 131.3, 127.3, 127.1, 123.0, 115.4, 106.3, 73.5, 70.6, 69.3, 31.9-21.0 (multi-carbon in alkyl chain), 14.1. Elemental analysis calcd (%) for $C_{56}H_{89}N_5O_4S$ (928.40); C 72.45, H 9.66, N 7.54; Found: C 72.39, H 9.63, N 7.56.
T3-14	Yellow solide；yield： 324 mg, 64%；^{1}H-NMR (400MHz, CDCl$_3$), δ (ppm): 7.92 (1H, d, Thio-H, *J* = 3.2 Hz), 7.59(2H, d, Ar-H, *J* = 8.5 Hz), 7.22 (1H, d, Thio-H, *J* = 3.2Hz), 7.00 (2H, d, Ar-H, *J* = 8.6 Hz), 6.62 (2H, s, Ar-H), 5.39 (4H, s, 2NH$_2$), 4.97 (2H, s, ArCH$_2$O), 3.99-3.93 (6H, m, 3ArOCH$_2$), 1.83-1.71 (6H, m, 3ArOCH$_2$C**H**$_2$), 1.46-1.26 (66H, m, 33CH$_2$), 0.88 (9H, t, 3CH$_3$, *J* = 6.9 Hz). ^{13}C-NMR (100MHz, CDCl$_3$), δ (ppm): 167.9, 167.1, 159.1, 153.4, 149.5, 139.4, 138.1, 131.5, 131.4, 127.3, 127.1, 123.1, 115.4, 106.2, 73.5, 70.6, 69.2, 31.9-22.7 (multi-carbon in alkyl chain), 14.1. Elemental analysis calcd (%) for $C_{62}H_{101}N_5O_4S$ (1012.56); C 73.54, H 10.05, N 6.92; Found: C 73.68, H 10.03, N 6.90.
T3-16	Yellow solide；yield：318 mg, 58%；^{1}H-NMR (500MHz, CDCl$_3$), δ (ppm): 7.93 (1H, d, Thio-H, *J* = 4.0 Hz), 7.61 (2H, d, Ar-H, *J* = 8.7 Hz), 7.24 (1H, d, Thio-H, *J* = 4.0 Hz), 7.01 (2H, d, Ar-H, *J* = 8.7 Hz), 6.62 (2H, s, Ar-H), 5.23 (4H, s, 2NH$_2$), 4.98 (2H, s, ArCH$_2$O), 3.99-3.94 (6H, m, 3ArOCH$_2$), 1.80-1.73 (6H, m, 3ArOCH$_2$C**H**$_2$), 1.46-1.25 (78H, m, 39CH$_2$), 0.88 (9H, t, 3CH$_3$, *J* = 6.5 Hz). ^{13}C-NMR (125MHz, CDCl$_3$), δ (ppm): 167.6, 166.2, 159.8, 153.8, 149.4, 139.2, 138.7, 132.8, 131.9, 127.9, 127.2, 123.8, 115.8, 106.7, 73.9, 71.0, 69.7, 32.3-23.1 (multi-carbon in alkyl chain), 14.5. Elemental analysis calcd (%) for $C_{68}H_{113}N_5O_4S$ (1096.72); C 74.47, H 10.39, N 6.39; Found: C 74.62, H 10.37, N 6.38.

3. References

S1 A. Immirzi, B.Perini, *Acta Cryst. Sect. A* 1977, **33**, 216–218.

S2 A. I. Kitaigorodsky, *Molekülkristalle*, Akademieverlag Berlin, 1979.

S3 X. H. Cheng, F. W. Su, R. Huang, H. F. Gao, M. Prehm, C. Tschierske, *Soft Matter*, 2012, **8** , 2274-2285.

S4 Y. Huang, Z. W. luo, X. H. Cheng, C. Tschierske, *Liq. Cryst.*, 2009, **36**, 61–66.